Iranian Journal of Basic Medical Sciences
ijbms.mums.ac.ir

Improved bioavailability of raloxifene hydrochloride through nasal administration of poly (methyl vinyl ether-co-maleic acid) nanoparticles in ovariectomized rats

Ladan Dayani [1], Jaleh Varshosaz [1]*, Mohsen Minaiyan [2]

[1] Novel Drug Delivery Systems Research Center, Department of Pharmaceutics, School of Pharmacy, Isfahan University of Medical Sciences, Isfahan, Iran
[2] Department of Pharmacology, School of Pharmacy and Pharmaceutical Sciences, Isfahan University of Medical Sciences, Isfahan, Iran

ARTICLE INFO

Article type:
Original

Article history:
Received: Aug 3, 2025
Accepted: Oct 29, 2025

Keywords:
Nasal delivery
Ovariectomized rats
Pluronic
Poly (Methyl vinyl ether-co-maleic acid) nanoparticles
Raloxifene hydrochloride
Thermoreversible gels

ABSTRACT

Objective(s): To improve the low bioavailability of Raloxifene hydrochloride (RH), which is just 2% through oral administration, an in situ mucoadhesive thermoreversible gel loaded with RH nanoparticles was formulated using Pluronic F127.

Materials and Methods: Mucoadhesion of the gels was modulated using Carbopol 934, Xanthan gum, and HPMC K4M as mucoadhesive polymers. The formulations containing 18% Pluronic and 0.2% Xanthan gum or 0.5% HPMC were considered as the optimized formulation based on their pH, gelation temperature, mucoadhesive strength, gel strength, viscosity, drug content, histopathological, and pharmacodynamic studies in ovariectomized rats.

Results: The gelation temperatures were 33.63±0.38 °C for Xanthan gum (0.2%) and 37.18±0.71 °C for HPMC (0.5%). Also, the 51758.67±62.17 dyn/cm^2 mucoadhesive strength was seen in HPMC 0.5% and 14867.33±192.60 dyn/cm^2 in Xanthan gum 0.2%. The drug released from the gel containing HPMC (0.5%) and Xanthan gum (0.2%) at 180 min was 98.2 ± 0.9% and 92.2 ± 5.6%, respectively. Serum calcium, phosphorus, and alkaline phosphatase significantly decreased in ovariectomized rats treated with oral estradiol valerate (as the standard treatment), and ovariectomized rats received nasal gels containing RH nanoparticles in comparison to the group with no treatment (P<0.05). Histopathological results indicated no adverse effects on the nasal mucosa following the administration of RH nanoparticle gels. Also, compared with the untreated drug, the nasal gel of RH nanoparticles showed an AUC0-24 that was 5.5-fold higher, indicating a significant improvement in RH relative bioavailability (P<0.05).

Conclusion: These results suggest that the thermoreversible nasal gel formulation of RH can be used as a safe drug-delivery system.

▶ Please cite this article as:
Dayani L, Varshosaz J, Minaiyan M. Improved bioavailability of raloxifene hydrochloride through nasal administration of poly (methyl vinyl ether-co-maleic acid) nanoparticles in ovariectomized rats. Iran J Basic Med Sci 2026; 29: 202-211. doi: https://dx.doi.org/10.22038/ijbms.2025.90740.19566

Introduction

Osteoporosis is an age-related disorder in humans defined by reduced bone mass and microarchitectural deterioration of bone tissue (1). It is recognized as a systemic skeletal disease associated with fragility fractures (2). The condition arises from insufficient postmenopausal estrogen levels, which regulate the activity of osteoblasts and osteoclasts (3). Multiple strategies have been employed for osteoporosis management, including hormone replacement and pharmacological therapy (4). Anabolic agents (e.g., parathyroid hormone) and anti-resorptive modifications are two common strategies for osteoporosis (5). Anti-resorptives are the primary pharmacological agents for osteoporosis, which inhibit osteoclast development and activity (6). One of them is raloxifene hydrochloride (RH, molecular weight of 510.05 g/mol), a second-generation non-steroidal benzothiophene selective estrogen receptor modulator (SERM) (7). RH has poor water solubility and an oral bioavailability of only 2% (8). In recent years, efforts have focused on enhancing the bioavailability of this drug. For example, Jha *et al.* (9) prepared raloxifene nanoparticles using milling and melt extrusion techniques to increase water solubility. Besides, Abukhalil (10) formulated the RH tablets using water-soluble diluents, including polyvinylpyrrolidone, anhydrous lactose, lactose monohydrate, crospovidone, hypromellose, modified pharmaceutical glaze, and propylene glycol, to enhance dissolution. Surfactants, including polysorbate 80, and super disintegrants, such as sodium starch glycolate, were also disclosed. In another patent, Alagarsamy *et al.* developed pharmaceutical formulations containing raloxifene, including its salts, esters, polymorphs, isomers, hydrates, and solvates (11).

***Corresponding author:** Jaleh Varshosaz. Novel Drug Delivery Systems Research Centre, Department of Pharmaceutics, School of Pharmacy and Pharmaceutical Sciences, Isfahan University of Medical Sciences, Isfahan, Iran. Tel: +98-3137927110, Fax: +98-3136680011, Email: varshosaz@pharm.mui.ac.ir

So, other delivery pathways, such as nasal delivery, seem to be an attractive alternative (12).

Nasal delivery enhances drug absorption through the nasal cavity and circumvents the hepatic first-pass effect (13). Due to the readily accessible vascular network, intranasal administration has emerged as a promising route for delivering medications directly into the bloodstream. The development of nasal formulations necessitates consideration of the physiologic characteristics of the nasal mucosa and the rapid mucociliary clearance of the nasal cavity (14). Drugs composed of small, lipophilic molecules with near-physiologic pH permeate membranes more efficiently (15). One of the primary limitations of nasal drug delivery is mucociliary clearance, which can be mitigated using thermoreversible gels (16, 17). Pluronic F127, an amphiphilic triblock copolymer, comprises hydrophobic polypropylene glycol units capped at each end with hydrophilic polyethylene glycol chains. These chains self-assemble via hydrophobic and hydrophilic interactions, forming a hydrophobic core surrounded by a hydrophilic shell. This material exhibits thermoreversible behavior. The potential of *in situ* gelation has shown encouraging results for drug delivery systems (18–20).

In our previous work, RH nanoparticles were fabricated by the electrospray technique using poly(methyl vinyl ether-co-maleic acid), were optimized, and were extensively characterized (21). RH nanoparticles demonstrated a tenfold increase in solubility compared with the free drug. The present study aimed to evaluate the nasal delivery of *in situ* gels containing RH nanoparticles as a novel drug delivery system, compared with RH nanoparticles alone, in ovariectomized rats.

Materials and Methods

The RH was kindly gifted by Iran Hormone Research Laboratories (Tehran, Iran). Poly (methyl vinyl ether-co-maleic acid) (Mw = 216000 Da) was purchased from Sigma Company (US). Pluronic (Lutrol F127), Carbopol 934P, HPMC K4M, Xanthan Gum, and all other reagents were obtained from Merck Chemical Company (Germany).

Preparation of RH nanoparticles by the electrospraying method

The electrospraying method was used to prepare RH nanoparticles. In summary, 130 mg of poly (methyl vinyl ether-co-maleic acid) and 6 mg of RH were dissolved in 1 ml of dimethylformamide. The collector of the electrospraying apparatus consisted of standard aluminum foil (17 × 21 cm^2) that served as the cathode. The clear solution was then transferred into a syringe fitted with a 23-gauge stainless steel nozzle, which served as the anode. Electrospraying conditions were set at a voltage of 18.24 kV, with a needle-to-collector distance of 19.69 cm and a flow rate of 0.43 ml/hr. The solution was extruded through the nozzle using a syringe pump (WPI, USA). Following electrospraying, the nanoparticles deposited on the collector were carefully collected, and the resulting dry powder was transferred into microtubes for subsequent analysis (21).

Preparation of thermo-reversible PF127 gels

Three levels of mucoadhesive polymers were evaluated: Carbopol 934P (0.1–0.3%), hydroxypropyl methylcellulose (HPMC K4M; 0.5–1.5%), and xanthan gum (0.1–0.3%). Aqueous solutions of 18% (w/v) Pluronic F127 containing the selected mucoadhesive agent and sufficient quantities of nanoparticles were prepared using the cold method described by Kim *et al.* (22). Briefly, mucoadhesive polymers and either nanoparticles or RH were added to deionized water and stirred continuously. Polymers were incorporated gradually into cold water under constant mixing. The resulting dispersions were stored at 4 °C overnight until clear solutions formed. Final formulations were assessed for pH, gelation temperature, mucoadhesive strength, gel strength, diffusion across sheep nasal mucosa, histopathological features, and pharmacodynamic activity in rats. The formulation of nasal gels of RH is presented in Table 1.

Characterization of gels

pH of formulation

The pH of each formulation was determined using a digital pH meter (Metrohm 827 pH Lab) after water dilution, which had been previously calibrated with phosphate buffers at pH 4 and 7.

Gelation temperature

Using a magnetic stirrer

Gelation temperature was measured by visual inspection (23). A 25 ml aliquot of each formulation was placed in a beaker on a magnetic stirrer at 25 °C. The temperature was monitored with a thermometer and increased by 2 °C per minute while stirring at 400 rpm. The temperature at which the magnetic bar ceased movement was recorded as the gelation temperature. Each measurement was performed in triplicate.

Using anton paar rheometer

To determine the gelation temperature by BROOKFIELD RVDVIII Rheometer (USA), 30 ml of the sample was used. Oscillation mode using temperature-sweep was employed at a constant rate from 25 °C to 40 °C. The shear stress was plotted against temperature with Rheoplus software.

Gel strength

The mechanical properties of the hydrogels were assessed by determining their elasticity coefficients using a pressure-based test. A defined amount of each hydrogel was positioned between the jaws of a tensile-strength apparatus (SANTAM STM1). The opposing jaw was lowered until contact was achieved. The force required to separate the

Table 1. Composition of different *in situ* nasal gels of raloxifene hydrochloride (RH)

Composition (% *w/v*)	T1	T2	T3	T4	T5	T6	T7	T8	T9
Pluronic F127	18	18	18	18	18	18	18	18	18
Corbopol 934	0.1	0.2	0.3	-	-	-	-	-	-
Xanthan Gum	-	-	-	0.1	0.2	0.3	-	-	-
HPMC K4M	-	-	-	-	-	-	0.5	1.0	1.5

jaws was recorded as the gel strength.

Mucoadhesive strength

Mucosal adhesion was assessed using a texture analyzer (BROOKFIELD CT3 4500, USA). Sheep nasal mucosa served as the membrane model for evaluating the mucosal adhesion of various formulations. Sections of mucosa (20 × 20 mm) were equilibrated at 37 °C for 15 min before mounting on the device. Each section was securely fixed to the probe. The probe was lowered at 0.5 mm/s until it contacted the gel, where a force of 1 N was maintained for 60 sec. The probe was then withdrawn at 0.5 mm/s over 15 mm (24). The texture analyzer, with CT V1.3 software, directly measured the maximum mass required to separate the probe from the tissue (expressed in grams).

$$\text{Adhesive mucous (dyne/cm}^2\text{)} = m \times g/A$$

In this equation, m is the mass required for separation in grams, g is the Gravitational acceleration (98 °cm-1s-2), and A is the cross-sectional area of the tissue.

Ex vivo permeation studies

Fresh nasal mucosa obtained from sheep at a local slaughterhouse was carefully excised and preserved in normal saline. After the removal of bone and cartilage, the mucosal membrane was prepared for testing (25). Franz diffusion cells were employed for evaluation. Before the experiment, the mucosa was equilibrated in phosphate buffer (pH 6.5, PBS) for 1 hour. Subsequently, the tissue was mounted on the receptor compartment of the Franz cell, and 4 ml of the gel formulation containing 879.64 µg of RH was uniformly applied to the donor surface.

Drug release was evaluated at 37 °C for 3 hr. The Franz cell receptor contained 27 ml of PBS (pH 6.5) and was stirred at 400 rpm. Samples were collected at 30, 45, 60, 90, 105, 135, 165, and 180 min. After UV absorbance measurement, the samples were returned to the medium. Absorbance was determined using a spectrophotometer (UV-mini 1240, Shimadzu, Kyoto, Japan) at 290 nm (26). Each formulation was tested in triplicate, and mean ± SD values of the percentage drug release were calculated. To characterize the release mechanism, *in vitro* release data were fitted to zero-order, first-order, Higuchi, and Korsmeyer–Peppas models.

Animal study

After optimizing the formulation, the effect of the best formulation was determined through nasal delivery in ovariectomized rats. For this purpose, 42 adult female Wistar rats (200–250 g) were randomly assigned to 7 experimental groups (n=6 per group). Animals were housed under standard laboratory conditions in accordance with European Community regulations for laboratory animals (ambient temperature 25 ± 2 °C, 12 hr dark/light cycle). The institutional animal ethical committee approved all protocols, and chow pellets and water were provided ad libitum. Group 1 consisted of intact animals (unovariectomized, untreated). Group 2 included ovariectomized animals without treatment. Group 3 comprised animals that were ovariectomized and then treated by oral administration of estradiol valerate (1 mg/kg per day). In group 4, rats were ovariectomized, then treated by nasal delivery of nanoparticles dissolved in normal saline, and then administered using a micropipette (0.1 mg/kg per day). In group 5, animals were ovariectomized, and blank gel containing 0.5% HPMC and 18% Pluronic F127 was administered 4 times a day. In group 6, ovariectomized rats were treated with nasal delivery of gel containing pure drug dispersion (0.1 mg/kg per day). Group 7 consisted of ovariectomized rats that were nasally delivered gels with RH nanoparticles using a micropipette (0.1 mg/kg per day) (optimized electrosprayed nanoparticles). For ovariectomy, they were anesthetized using intraperitoneal ketamine HCl and xylazine injection at doses of 50 mg/kg and 10 mg/kg body weight, respectively. Then, their abdomens were shaved, and the skin was disinfected with 70% ethanol, followed by povidone-iodine (Betadine) solution. Bilateral ovariectomy was performed through a dorsal midline incision just caudal to the 13th rib. Bilateral dorsal incisions were made on the back to locate the ovaries. The procedure involved ligation of ovarian arteries, cutting the connection between the fallopian tube and the uterine horn, and excision of the ovaries. Finally, the muscle layer and the skin incision were closed using silk suture. Twenty-six days after ovariectomy, serum calcium (Ca), phosphorus (P), and alkaline phosphatase (ALP) levels were measured. Then, they were treated for 60 days, and serum Ca, P, and ALP levels were measured using commercial detection kits (Pars Azmoon Co. and BioRexFars Co.). Handling of animals and experimental procedures were performed according to the Guide for the Care and Use of Laboratory Animals by the National Institutes of Health (USA) (publication No. 85-23, revised 1996) and the current laws of the Iranian government. All protocols for animal experiments were approved by the institutional animal ethics committee.

Histopathological evaluation of mucosa

Following the animal studies, Hematoxylin and Eosin staining of the nasal mucosa was performed. Rats from the nasal nanoparticle gel group (Group 7) and the nasal nanoparticle powder group (Group 4) were euthanized using ether. The median portion of the septum was excised and immersed in 6% formaldehyde. Histopathological evaluation of tissue incubated in PBS (pH 6.5) was compared with tissue incubated in the diffusion chamber containing the gel formulation. Nasal tissues were fixed in 10% buffered formalin, embedded in paraffin, sectioned at 5 µm, and stained with hematoxylin and eosin (H&E). Sections were examined under light microscopy for evidence of tissue damage (27). Additionally, three healthy rats received intranasal deoxycholate for one week to confirm mucosal injury. This group served as a control for comparing nasal tissue with that of the experimental groups.

Pharmacokinetic studies

Fasted healthy female Wistar rats (200–250 g) were deprived of food for 12 hr before and 4 hr after drug administration, but had free access to water. Animals were divided into two groups (n=6 per group): one received an oral single dose of pure drug (15 mg/kg) using an oral gavage needle, and the other received nasal RH nanoparticle gel containing 0.5% HPMC and 18% Pluronic F127 (28). Ether anesthesia was administered before retro-orbital blood sampling with heparinized capillaries. Blood samples (0.5 ml) were collected at 0.083, 0.25, 0.5, 1.0, 2, 4, 8, 12, and 24 hr. Samples were centrifuged at 10,000 rpm for 15 min, and plasma was separated and stored at −20 °C until analysis by HPLC.

Table 2. Results of gel strength, gelation temperature, and pH of different formulations (n=3)

Composition (%*w/v*)			Gel strength (N)	Gelation temperature (°C)	pH
T1		0.1	9.5 ± 0.7	31.9±0.8	5.2±0.2
T2	Corbopol 934	0.2	18.4± 1.0	30.7 ± 1.6	4.7±0.1
T3		0.3	17.9 ± 1.1	29.1 ± 1.6	4.2±0.3
T4		0.1	15.8 ± 0.4	32.8± 1.5	6.4±0.2
T5	Xanthan gum	0.2	15.3± 0.6	34.7 ± 0.7	6.7±0.2
T6		0.3	14.6 ± 0.5	31.4 ± 1.9	6.6±0.4
T7		0.5	23.1 ± 0.9	37.2 ± 0.4	6.7±0.5
T8	HPMC K4M	1.0	50.9± 2.1	30.1 ± 0.6	6.7±0.2
T9		1.5	53.5± 3.7	25.9 ± 0.7	6.8±0.1

Plasma sample preparation

For plasma preparation, 100 µl of methanol and 300 µl of acetonitrile were added to 100 µl of plasma, and the mixture was vortex-mixed for 10 seconds. Denatured proteins were removed by centrifugation at 15,000 rpm for 10 min. A 20 µl aliquot of the supernatant was injected into the HPLC for analysis. The pharmacokinetic parameters, including C_{max}, T_{max}, AUC_{0-24}, $AUC_{0-\infty}$, K_a, and K_{el}, were calculated for both the pure drug and RH nanoparticles.

HPLC analysis method

Drug plasma concentrations were measured using a reversed-phase HPLC (Waters, 5.5, USA) system with two pumps and a UV detector. Mobile phase consisted of acetonitrile, ammonium acetate (pH 4.0, 0.05 M) (50:50 v/v%) with a flow rate of 0.8 ml/min to elute the drug that was filtered through 0.22 μm nylon filters (Millipore, USA). The samples were analyzed at λ_{max} 289 nm.

Statistical analysis

Data were analyzed using analysis of variance (ANOVA) followed by a *post hoc* test using LSD, and results were presented as mean ± SD.

Results

Evaluation of formulations

pH

Table 2 shows the pH results for formulations prepared with Carbopol 934, HPMC K4M, and Xanthan gum. As seen, the pH ranges in all formulations are between 4.2±0.3 and 6.85±0.1. The Carbopol formulations showed acidic pH, which was unsuitable for nasal administration. However, the pH of the other formulations was appropriate for nasal application.

Gelation temperature

According to the results presented in Table 2, gelation temperature ranged from 25.9 to 37.2 °C. Increasing HPMC concentration significantly reduced Tsol–gel (P<0.05), whereas no significant effect was observed for other mucoadhesive agents (P>0.05). High concentrations of HPMC and Carbopol were unsuitable for administration. The average nasal cavity temperature is approximately 34 °C (29); therefore, formulations with $T_{sol-gel}$ near or slightly above this value were selected for further investigation. Results indicated that 0.5% HPMC and 0.2% xanthan gum exhibited $T_{sol-gel}$ values within the physiological range (Table 2).

As shown in Table 3, rheometric analysis determined that the Tsol-gel temperature was 37.18 °C for 0.5% HPMC and 33.63 °C for 0.2% xanthan gum. Figure 1 illustrates the gelation temperature profiles for these two formulations. Shear stress increased sharply at Tsol-gel, confirming the sol-to-gel transition (30). These findings were consistent with gelation temperatures determined by visual inspection.

Gel strength

Gel strength values for the various formulations are presented in Table 2. Increasing mucoadhesive polymer concentration significantly enhanced gel strength (P<0.05), except for 0.1% and 0.2% xanthan gum. HPMC had a greater effect on gel strength than the other agents (P<0.05), in agreement with previous studies (31).

Mucoadhesive strength

The mucoadhesive strengths of 0.2% xanthan gum

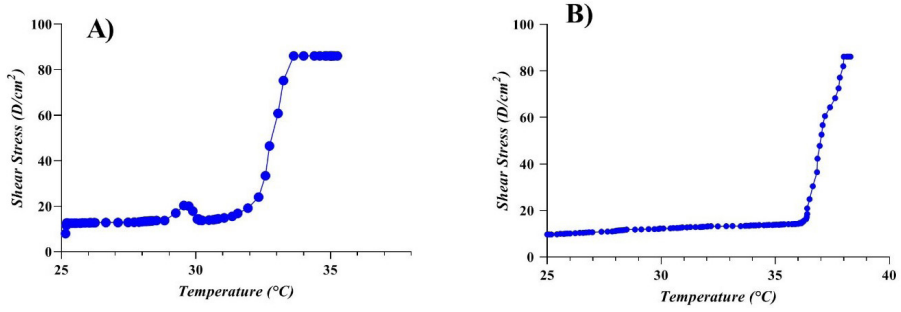

Figure 1. Graphs of the gelation temperature. A) 0.2 % Xanthan gum B) 0.5 % HPMC
HPMC: Hydroxypropyl methylcellulose

Table 3. The gelation temperature and mucoadhesive strength of 0.2% xanthan gum and 0.5% hydroxypropyl methylcellulose (HPMC) formulations.

Formulation	Gelation temperature (˚C)	Mucoadhesive strength (dyn/cm²)
0.2 % Xanthan gum	33. 63±0.38	14867.33±192.60
0.5 % HPMC	37.18±0.71	51758.67±62.17

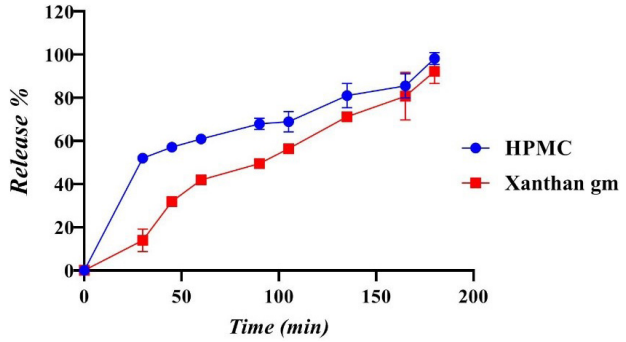

Figure 2. Cumulative release percent of RH from 0.5% hydroxypropyl methylcellulose (HPMC) and 0.2% xanthan gum gel formulations. Values are expressed as mean ± SD (n=3).

and 0.5% HPMC were 14867.33 ± 192.60 and 51758.67 ± 62.17 dyn/cm², respectively (Table 3). As shown, HPMC demonstrated significantly higher mucoadhesive strength than xanthan gum (P<0.05), consistent with earlier reports (32, 33).

Ex vivo permeation studies

The *ex vivo* permeation profiles of *in situ* nasal gels containing 0.5% HPMC and 0.2% xanthan gum across the nasal mucosa are presented in Figure 2. Profiles were obtained by plotting drug release percentage versus time. Approximately 90% of the drug permeated the nasal mucosa within 180 min for both formulations. Results indicated that the gels retained RH throughout the 180 min. In earlier studies, more than 99% of RH dissolved within 30 min; however, at the 30-minute time point, 52.05 ± 0.7% and 13.9 ± 5.3% of the drug were released from 0.5% HPMC and 0.2% xanthan gum gels, respectively. The *in situ* gels significantly retarded drug release compared with nanoparticles (P<0.05). According to Table 4, drug release percentages at 180 min were 98.2 ± 0.9% for 0.5% HPMC and 92.2 ± 5.6% for 0.2% xanthan gum. Corresponding RE% values were 61.8 ± 2.1 and 45.3 ± 0.7, respectively.

Coefficient values for different formulations of nasal *in situ* RH gels are presented in Table 5. For 0.5% HPMC, correlation coefficients were 0.9573 for the Higuchi model, 0.9172 for the first-order model, and 0.7842 for the zero-order model. For 0.2% xanthan gum, correlation coefficients were 0.9381 for the Higuchi model, 0.9477 for the first-order model, and 0.9779 for the zero-order model (Table 5).

Animal studies

Serum calcium, phosphorus, and alkaline phosphatase (ALP) levels

The effects of nasal delivery of nanoparticles and thermoreversible gels containing nanoparticles on serum calcium, phosphorus, and ALP levels in ovariectomized rats are shown in Figure 3. Serum calcium levels were significantly

Table 4. The drug release of the 0.5% hydroxypropyl methylcellulose (HPMC) and 0.2% xanthan gum gels. Values are expressed as mean ± SD (n=3)

Formulation	Time (min)	% Drug release ± SD	RE% ± SD
0.5 % HPMC	180	98.2 ± 0.9	61.8 ± 2.1
0.2 % Xanthan gum	180	92.2 ± 5.6	45.3 ± 0.7

Table 5. The fitting results of *in vitro* release for 0.5% hydroxypropyl methylcellulose (HPMC) and 0.2% xanthan gum gels

Formulation	Higuchi	First order	Zero order	Korsmeyer-Peppas
0.5 % HPMC	Y = 6.3061X+ 10.684	Y = -0.0042X + 2.8231	Y = 0.3886X + 27.891	Y = 0.3096X + 1.2424
	R^2= 0.9573	R^2= 0.9172	R^2= 0.7842	R^2= 0.9555
0.2 % Xanthan	Y = 6.9947X - 11.597	Y = -0.0044X + 2.991	Y = 0.4862X + 4.9081	Y = 0.9213X - 0.1032
	R^2= 0.9381	R^2= 0.9477	R^2= 0.9779	R^2= 0.9411

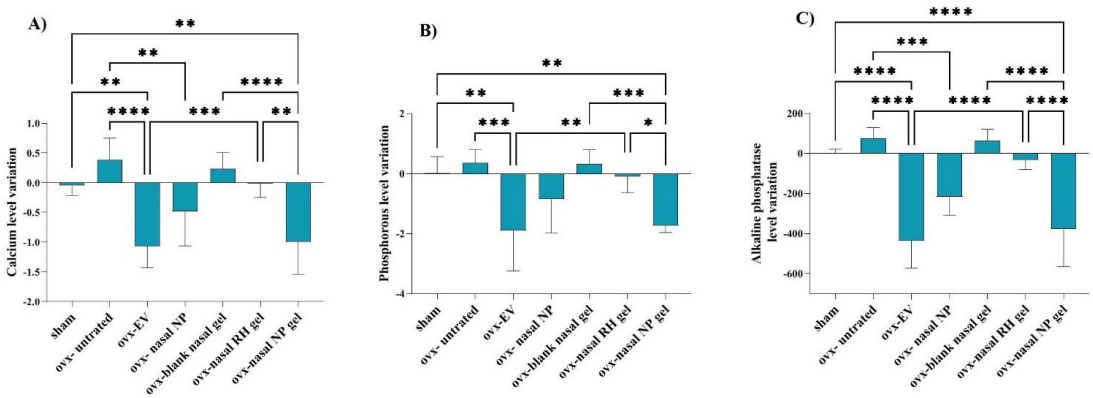

Figure 3. The effect of different studied groups of nasal raloxifene hydrochloride nanoparticle, and nasal raloxifene hydrochloride nanoparticle gel on serum A) Calcium B) Phosphorus C) ALP in ovariectomized rats (n=6)
ALP: Alkaline phosphatase

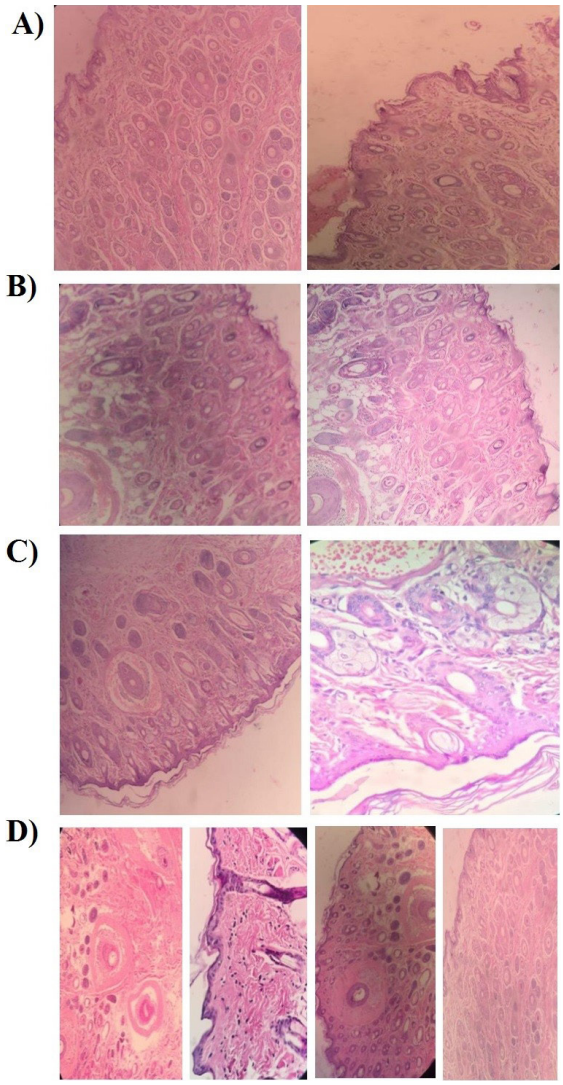

Figure 4. H & E staining of nasal mucosa sections for rats received A) Nasal delivery of RH nanoparticle gel B) Nasal delivery of nanoparticle powder C) Normal saline D) Sodium deoxycholate. Magnification × 400.
RH: Raloxifene hydrochloride

elevated in untreated ovariectomized rats compared with normal controls (Figure 3A) (P<0.05). In contrast, calcium levels were significantly reduced in ovariectomized rats treated with nasal gels containing pure drug compared with untreated ovariectomized controls and blank nasal gels (P<0.05). Serum calcium was also significantly reduced in ovariectomized rats treated with estradiol valerate or nasal gels containing RH nanoparticles compared with other groups (Figure 3A) (P<0.05). No significant difference was observed between ovariectomized rats treated with nasal gels containing RH nanoparticles and those receiving oral estradiol (P>0.05). A significant difference was noted between rats treated with nasal nanoparticles and those treated with estradiol valerate (P<0.05), while no difference was observed between the nasal nanoparticle and nasal nanoparticle gel groups (P>0.05).

According to the results, serum phosphorus levels were significantly reduced in ovariectomized rats treated with estradiol valerate, nasal nanoparticle powder, or nasal gels containing nanoparticles compared with untreated ovariectomized controls and blank nasal gel (Figure 3B) (P<0.05). No significant differences were observed among ovariectomized rats treated with RH nanoparticle gels, nasal nanoparticles, or oral estradiol valerate (P>0.05). A significant reduction was also noted in the ovariectomized group treated with nasal gels containing pure drug compared with untreated ovariectomized rats (P<0.05).

As shown in Figure 3C, serum ALP activity was markedly reduced in ovariectomized rats treated with estradiol valerate, nasal nanoparticle powder, or nasal gels containing nanoparticles compared with other groups (P<0.05). No significant difference was observed between ovariectomized rats treated with RH nanoparticle gels and those treated with estradiol valerate (P>0.05). However, a significant difference was observed between the nasal nanoparticle powder group and the estradiol group (P<0.05).

Histopathological studies

Histopathological examination demonstrated that RH had no adverse local effects on the nasal mucosa of rats treated with nasal nanoparticles or gels containing nanoparticles. As shown in Figure 4C, the normal nasal mucosa of untreated rats was lined with intact olfactory epithelium. In contrast, the sodium deoxycholate group exhibited complete epithelial disruption, fibrosis, and infiltration of inflammatory cells (Figure 4D). In contrast, epithelial tissues from rats treated with nasal gels or nanoparticles (Figures 4A and 4B) showed no structural alterations, and microscopic examination revealed no detectable mucosal damage in these groups.

Pharmacokinetic studies

Serum concentration–time profiles of untreated RH and nasal gels containing RH nanoparticles are shown in Figure 5, indicating a two-compartment pharmacokinetic model. Significant differences in C_{max}, T_{max}, AUC_{0-24}, $AUC_{0-\infty}$, K_{el}, and K_a were observed between RH nanoparticles and the untreated drug at equivalent doses (P<0.05) (Table 6). Rats receiving nasal gels of RH nanoparticles exhibited C_{max} and K_a values of 5.22 ± 1.09 µg/ml and 3.55 ± 0.79 h^{-1}, respectively, compared with 0.485 ± 0.13 µg/ml and 0.29 ± 0.10 h^{-1} for oral RH. The enhanced dissolution rate, solubility, and reduced crystallinity of RH, attributed to the increased surface area of nanoparticles and reduced particle size, explain the higher blood concentrations and shorter T_{max} observed with RH nanoparticles compared with the untreated drug. Nasal gels containing RH nanoparticles achieved a 5.5-fold greater AUC_{0-24} than untreated RH, demonstrating a significant improvement in relative bioavailability (P<0.05).

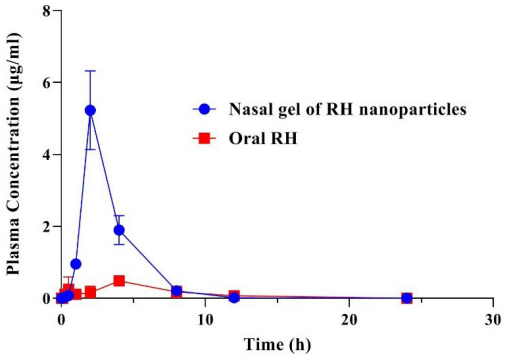

Figure 5. Plasma concentration-time profiles of RH after oral administration of 15 mg/kg pure RH powder and equivalent amounts of nasal RH nanoparticles gel in rats (n=6)
RH: Raloxifene hydrochloride

Table 6. Pharmacokinetic parameters of oral RH in comparison to the nasal gel of RH nanoparticles

RH type	C_{max} (µg/ml)	T_{max} (min)	K_a (h^{-1})	K_{el} (h^{-1})	AUC_{0-24} (µg.h/ml)	$AUC_{0-\infty}$ (µg.h/ml)
Oral RH	0.48±0.13	240.0±0.0	0.29±0.10	0.017±0.006	3.19±0.87	3.19±0.87
Nasal gel of RH nanoparticles	5.22±1.09*	120.0±0.0*	3.55±0.79*	0.009±0.005	15.29±2.66*	16.72±2.01*

Note: Each value represents the mean ± SD (n=6)

*$P<0.05$ shows significant difference compared with pure RH powder. RH: Raloxifene hydrochloride

Discussion

One strategy to reduce rapid mucociliary clearance is the use of mucoadhesive formulations, which prolong residence time at the nasal absorption site and enhance drug uptake (34). Previous studies have reported that poloxamer solutions undergo phase transition to bioadhesive gels at body temperature (35). In this study, Pluronic F127 was employed to achieve this objective.

ormulations containing nanoparticles appeared clear, with no visible particles, indicating favorable syringeability. In contrast, gels prepared with pure RH were not translucent and precipitated within 24 hr, likely because nanoparticles were more soluble than the drug. Three types of gels incorporating different mucoadhesive agents (HPMC, Carbopol 934, and xanthan gum) were prepared, each containing 18% (w/v) Pluronic F127. Gel strength, gelation temperature, and pH values for these formulations are summarized in Table 2.

The mucus layer covering the olfactory and respiratory mucosa represents the first barrier encountered by intranasally administered pharmacological agents (36). The pH of nasal mucus typically ranges from 5.5 to 6.5 (37). Maintaining pH within this range is critical (38). Under alkaline conditions, lysosomal secretion from nasal cells is inhibited, rendering the tissue more susceptible to microbial infection. Conversely, formulations with a pH below three may cause intracellular damage and, by acting as hypertonic solutions, can lead to epithelial cell shrinkage and suppression of ciliary activity (39, 40). Accordingly, it was essential to ensure that formulation pH remained within the physiologic range to prevent pH-related mucosal irritation. In this study, the pH values of the formulations ranged from 4.2 to 6.8 (Table 2). No irritation was anticipated for formulations within the physiological range, except for those containing higher concentrations of Carbopol. These acidic solutions, produced by increasing Carbopol concentration, were deemed unsuitable for use. Balakrishnan *et al.* (41) employed Carbopol for intranasal delivery but did not report solution pH; however, their formulations included 0.1% Carbopol. In our study, a 0.1% Carbopol solution had a pH of 5.2 ± 0.2, within the physiological range.

The temperature at which an aqueous solution transitions to a hydrogel is called the gelation temperature or sol–gel transition temperature (Tsol-gel). Below this threshold, the formulation remains fluid-like and suitable for administration. If the gelation temperature is excessively high, the formulation remains liquid under physiological conditions. In contrast, if it is too low, the formulation becomes viscous before instillation and fails to meet nasal delivery requirements. Therefore, a range of 32–38 °C is considered optimal for gel formation upon exposure to body temperature (42, 43). According to Table 2, the gelation temperatures of the xanthan gum and HPMC K4M formulations fell within this range. Previous reports indicated that increasing the Pluronic concentration lowers the sol–gel transition temperature; therefore, a fixed concentration of 18% Pluronic was used (44), and mucoadhesive agents were subsequently added to achieve the desired gelation profile. The mechanism of poloxamer gelation has been described in earlier studies. Poloxamers exhibit thermoreversible behavior due to a negative solubility coefficient. At lower temperatures, poloxamers dissolve readily in water. As the temperature increases to a critical point, molecules undergo self-assembly into spherical micelles, consisting of a hydrophobic polypropylene oxide core surrounded by hydrophilic polyethylene oxide chains. Thermoreversible gelation occurs through multimolecular aggregation and micellar entanglement as the temperature rises (45, 46). According to Table 2, formulations with low gel strengths degrade rapidly, whereas those with high gel strengths are not good, as the gels are too firm to deliver. The suitable values of gel strength are easy to administer, and postnasal drip does not occur (47).

Sherafudeen SP et al. (33) prepared formulations with varying polymeric ratios of HPMC K-100 and xanthan gum. Their findings demonstrated that HPMC K-100 produced greater mucoadhesive strength than xanthan gum. Consequently, increased mucoadhesion and gel strength were expected to extend nasal residence time (48). These findings are consistent with our results presented in Table 3.

As indicated by the drug release profiles (Figure 2), each formulation exhibited an initial burst release during the first minutes, likely due to incomplete gel formation (44). An inflection point was observed during the sol–gel transition, after which the rate of drug release slowed. As shown in Figure 2, the 0.5% HPMC formulation demonstrated a comparatively higher release rate than the 0.2% xanthan gum formulation, although both displayed nearly identical overall profiles. This similarity may be attributed to the common base polymer, Pluronic F127, used at 18% in both formulations, with low concentrations of mucoadhesive agents exerting minimal effect on release kinetics. This observation could explain the comparable drug release patterns despite differences in mucoadhesive polymers (44). The higher release rate observed with HPMC compared to xanthan gum may be due to differences in their molecular structures and concentrations. The methoxy groups in HPMC exert less influence on polymer viscosity, resulting in increased drug release (49).

When hydrophilic polymers come into contact with aqueous media, they form a hydrated gel layer that acts as a barrier to drug diffusion. The thickness of this hydrated layer governs the rate of molecular release from the matrix. In addition, drug release is influenced by the degree of swelling and erosion of the hydrated polymer (49).

From the results in Table 5, it is concluded that RH release from a 0.5 % HPMC-based gel followed Higuchi

kinetics, indicating a diffusion process. In contrast, for 0.2 % xanthan gum, it followed a zero-order mechanism. Charoo *et al.* (50) showed that the release of ciprofloxacin from a system containing Carbopol and HPMC followed zero-order kinetics, and the base showed excellent antimicrobial activity. Its shelf life has been reported to exceed 2 years. In another study, cilostazol was released from the Carbopol-Pluronic base using the Diffusion method (51).

Serum calcium, phosphate, and ALP levels are related to osteoporosis (52). In normal conditions, a balance between osteoclastic bone resorption and osteoblastic bone formation exists, guaranteeing stable bone mass. By the reduction of estrogen, postmenopausal osteoporosis occurs, leading to a sharp acceleration of bone turnover. In this regard, body mass density (BMD) and biochemical parameters are considered the most common and easiest tools for estimation of osteoclastic activity (53). By lowering BMD, inactive osteoblasts are triggered, resulting in unmineralized bone-like tissue and undifferentiated osteoblasts. Thus, serum calcium and phosphorus levels increase. Also, ALP levels are regulated in a feedback loop with osteoblast proliferation (54, 55). Pardhe *et al.* (53) proved that the mean value of serum phosphorus and ALP levels was significantly increased ($P<0.05$) in postmenopausal women when compared to premenopausal women. Nasal administration of RH encapsulated in poly (methyl vinyl ether-co-maleic acid) nanoparticles embedded within a mucoadhesive hydrogel significantly improved serum biochemical parameters in female Wistar rats. Serum calcium, phosphorus, and ALP levels were markedly reduced in ovariectomized rats treated with RH gels (Figure 3). As shown in Figures 3A–C, ovariectomy increased serum calcium, phosphorus, and ALP levels in untreated animals. In contrast, rats receiving RH-loaded nanoparticles in gel exhibited significant reductions in these parameters compared with the untreated and previous control groups ($P<0.05$). Reductions in calcium and phosphorus levels in the positive control group (treated with estradiol valerate) were greater than in the group treated with nasal RH gels ($P<0.05$).

Histological analysis demonstrated that normal rat nasal mucosa exhibited neither necrosis nor epithelial detachment. No alterations were observed in the epithelial or basal layers of groups treated with RH gels or nanoparticles when compared with untreated controls. These findings suggest that the formulations are safe for nasal administration (Figure 4).

As illustrated in Figure 5, enhanced solubility contributed to a substantial increase in RH bioavailability. Pharmacokinetic results (Table 6) revealed a fivefold increase in $AUC_{0-\infty}$ for RH nanoparticles compared with the untreated drug. Ahmed *et al.* (56) developed misemulsions containing micelles composed of vitamin E and D-α-tocopheryl polyethylene glycol 1000 succinate in nanosized self-emulsifying systems, reporting a 4.79-fold increase in bioavailability compared to control nasal gels and a 13.42-fold increase compared with oral tablets in rats. Similarly, Saini *et al.* (57) demonstrated that intranasal administration of RH-loaded chitosan nanoparticles, prepared by ionic gelation, resulted in higher plasma drug concentrations compared with oral RH suspensions.

In summary, the prepared system suitably controlled the drug release and could be administered nasally by instillation. Upon exposure to body temperature, the prepared gel could undergo a sol-gel transition, prolonging resistance time in the nasal cavity and ensuring nasal absorption of RH, as confirmed by the pharmacokinetics results. This system was first used for nasal administration of RH. Moreno *et al.* (58) used Pluronic F 127 and PMVEMA to prepare copolymers for controlled protein release. Also, this system was employed to produce micelles for doxorubicin delivery in breast cancer (59).

Conclusion

In summary, this study indicates that ovariectomized rats treated with RH nanoparticle nasal powder, as well as those receiving RH nanoparticle nasal gels, exhibited improved pharmacodynamic activity compared with pure RH. The results also indicated that nasal gels of RH nanoparticles significantly enhanced the bioavailability of the orally administered RH. Therefore, we propose that nasal administration enhances the bioactivity of the RH. Nonetheless, we believe additional research is necessary to explore all facets of nasal delivery of the RH for potential clinical applications.

Acknowledgment

The authors would like to acknowledge the financial support of Isfahan University of Medical Sciences, Iran.

Ethical Statement

All animal experiments complied with the ARRIVE guidelines and were carried out in accordance with the National Institutes of Health guide for the care and use of Laboratory animals (NIH Publications No. 8023, revised 1978). The guidelines for animal research established by the Isfahan University of Medical Sciences ethical committee were followed (ethical code: IR.MUI.REC.1394.3.690), in accordance with the NIH Guide for the Care and Use of Laboratory Animals.

Availability of Data and Materials

Data are available on request.

Funding

Isfahan University of Medical Sciences financially supports the (Project number: 394690).

Authors' Contributions

J V Design of the work and supervision, L D data collection analysis and writing of the article, M M supervision and validation. All authors of the present study participated in different stages and shared ideas.

Conflicts of Interest

The authors declare no conflict of interest.

Declarations

We have not used any AI tools or technologies to prepare this manuscript.

References

1. Walker MD, Shane E. Postmenopausal osteoporosis. N Engl J Med 2023; 389:1979–1991.
2. Aibar-Almazán A, Voltes-Mart\'\inez A, Castellote-Caballero Y, Afanador-Restrepo DF, Carcelén-Fraile M del C, and López-Ruiz E. Current status of the diagnosis and management of osteoporosis.

Int J Mol Sci 2022; 23:9465-9491.
3. Anam AK, Insogna K. Update on osteoporosis screening and management. Med Clin 2021; 105:1117–1134.
4. Foessl I, Dimai HP, and Obermayer-Pietsch B. Long-term and sequential treatment for osteoporosis. Nat Rev Endocrinol 2023; 19:520–533.
5. Song S, Guo Y, Yang Y, and Fu D. Advances in pathogenesis and therapeutic strategies for osteoporosis. Pharmacol Ther 2022; 237:108168.
6. Zhang L, Zheng Y-L, Wang R, Wang X-Q, and Zhang H. Exercise for osteoporosis: a literature review of pathology and mechanism. Front Immunol 2022; 13:1005665.
7. Alyamani M, Alshehri S, Alam P, Wani SUD, Ghoneim MM, Shakeel F. Solubility and solution thermodynamics of raloxifene hydrochloride in various (DMSO+ water) compositions. Alexandria Eng J 2022; 61:9119–9128.
8. Kher JD, Sorathia K, and Kher JD. Bioavailability enhancement of BCS class II raloxifene hydrochloride by inclusion complex and solid dispersion techniques. Zhongguo Ying Yong Sheng Li Xue Za Zhi= Zhongguo Yingyong Shenglixue Zazhi= Chinese J Appl Physiol 2024; 40:e20240002.
9. Jha AK. Methods of improving the solubility and bioavailability of therapeutic agents. United States: Google Patents; US11311493B2, 2025.
10. Abukhalil A. Raloxifene composition. WIPO (PCT); WO2011000581A2, 2011.
11. Alagarsamy A, Rambabu B, Reddy PS, Venugopal K, Kumar BR. Raloxifene pharmaceutical formulations. United States; US20110159084A1, 2009.
12. Williams G, Suman JD. *In vitro* anatomical models for nasal drug delivery. Pharmaceutics 2022; 14:1353-1364.
13. Chavda VP, Jogi G, Shah N, Athalye MN, Bamaniya N, Vora LK, *et al.* Advanced particulate carrier-mediated technologies for nasal drug delivery. J Drug Deliv Sci Technol 2022; 74:103569.
14. Rai G, Gauba P, Dang S. Recent advances in nanotechnology for Intra-nasal drug delivery and clinical applications. J Drug Deliv Sci Technol 2023; 86:104726.
15. Rabiee N, Ahmadi S, Afshari R, Khalaji S, Rabiee M, Bagherzadeh M, *et al.* Polymeric nanoparticles for nasal drug delivery to the brain: relevance to Alzheimer's disease. Adv Ther 2021; 4:2000076.
16. Keller L-A, Merkel O, and Popp A. Intranasal drug delivery: Opportunities and toxicologic challenges during drug development. Drug Deliv Transl Res 2022; 12:735–757.
17. Fortuna A, Schindowski K, and Sonvico F. Intranasal drug delivery: Challenges and opportunities. Front Pharmacol 2022; 13:868986.
18. Li S, Yang C, Li J, Zhang C, Zhu L, Song Y, *et al.* Progress in pluronic F127 derivatives for application in wound healing and repair. Int J Nanomedicine 2023; 18: 4485–4505.
19. Shamma RN, Sayed RH, Madry H, El Sayed NS, and Cucchiarini M. Triblock copolymer bioinks in hydrogel three-dimensional printing for regenerative medicine: A focus on pluronic F127. Tissue Eng Part B Rev 2022; 28:451–463.
20. Lupu A, Rosca I, Gradinaru VR, and Bercea M. Temperature induced gelation and antimicrobial properties of Pluronic F127 based systems. Polymers (Basel) 2023; 15:355-372.
21. Varshosaz J, Minaiyan M, and Dayyani L. Poly(methyl vinyl ether-co-maleic acid) for enhancement of solubility, oral bioavailability and anti-osteoporotic effects of raloxifene hydrochloride. Eur J Pharm Sci 2018; 112:195–206.
22. Kim EY, Gao ZG, Park JS, Li H, Han K. rhEGF/HP-beta-CD complex in poloxamer gel for ophthalmic delivery. Int J Pharm 2002; 233:159–167.
23. Qian L, Cook MT, Dreiss CA. *In situ* gels for nasal delivery: Formulation, characterization and applications. Macromol Mater Eng 2025; 2400356.
24. Suhagiya K, Borkhataria CH, Gohil S, Manek RA, Patel KA, Patel NK, *et al.* Development of mucoadhesive in-situ nasal gel formulation for enhanced bioavailability and efficacy of rizatriptan in migraine treatment. Results Chem 2023; 6:101010.
25. Hard SAAA, Shivakumar HN, Bafail DA, and Moqbel Redhwan MA. Development of *in vitro* and *in vivo* evaluation of mucoadhesive in-situ gel for intranasal delivery of vinpocetine. J Drug Target 2025; 33:528–545.
26. El-Shenawy AA, Mahmoud RA, Mahmoud EA, Mohamed MS. Intranasal in situ gel of apixaban-loaded nanoethosomes: Preparation, optimization, and *in vivo* evaluation. AAPS PharmSciTech 2021; 22:147. doi: 10.1208/s12249-021-02020-y.
27. Mali A, Bhanwase A. *In vitro*, *Ex vivo* and *in vivo* assessment of brain targeted thermoreversible mucoadhesive *in situ* intranasal gel of carmustine for the treatment of glioblastoma. Bionanoscience 2024; 14:2571–2581.
28. Shah N V, Seth AK, Balaraman R, Aundhia CJ, Maheshwari RA, Parmar GR. Nanostructured lipid carriers for oral bioavailability enhancement of raloxifene: Design and *in vivo* study. J Adv Res 2016; 7:423–434.
29. Tjahjono R and Singh N. Correlation between nasal mucosal temperature change and the perception of nasal patency: A literature review. J Laryngol Otol 2021; 135:104–109.
30. Zhou Y, Zhang X-L, Lu S-T, Zhang N-Y, Zhang H-J, Zhang J, *et al.* Human adipose-derived mesenchymal stem cells-derived exosomes encapsulated in pluronic F127 hydrogel promote wound healing and regeneration. Stem Cell Res Ther 2022; 13:407-423.
31. Wu T-Y, Huang C-C, Tsai H-C, Lin T-K, Chen P-Y, Darge HF, *et al.* Mucin-mediated mucosal retention via end-terminal modified Pluronic F127-based hydrogel to increase drug accumulation in the lungs. Biomater Adv 2024; 156:213722.
32. Morsi N, Ghorab D, Refai H, and Teba H. Ketoroloac tromethamine loaded nanodispersion incorporated into thermosensitive in situ gel for prolonged ocular delivery. Int J Pharm 2016; 506:57–67.
33. Sherafudeen SP and Vasantha PV. Development and evaluation of *in situ* nasal gel formulations of loratadine. Res Pharm Sci 2015; 10:466–476.
34. Srivastava SK, Prasad M, Jha AK. Development and Evaluation of Thermo Triggered *in situ* nasal gel of selegiline for depressive disorders: *In vitro*, *in vivo* and *ex vivo* characterization. Res J Pharm Technol 2022; 15:1424–1430.
35. Garc\'\ia-Couce J, Tomás M, Fuentes G, Que I, Almirall A, Cruz LJ. Chitosan/Pluronic F127 thermosensitive hydrogel as an injectable dexamethasone delivery carrier. Gels 2022; 8:44-59.
36. Nian X, Zhang J, Huang S, Duan K, Li X, Yang X. Development of nasal vaccines and the associated challenges. Pharmaceutics 2022; 14:1983-2008.
37. Mali AH, Shaikh AZ. A short review on nasal drug delivery system. Asian J Pharm Technol 2021; 11:289–292.
38. Amponsah SK and Adams I. Drug Absorption via the Nasal Route: Opportunities and Challenges. In: Nasal Drug Delivery, Formulations, Developments, Challenges, and Solutions, Springer International Publishing, 2023; 25–42.
39. Mankar SD, Parjane SR, Siddheshwar SS, Dighe SB. Formulation, optimization and *in vivo* characterization of thermosensitive *in situ* nasal gel loaded with bacoside a for treatment of epilepsy. AAPS PharmSciTech 2024; 25:151. doi: 10.1208/s12249-024-02870-2.
40. Kammoun AK, Khedr A, Hegazy MA, Almalki AJ, Hosny KM, Abualsunun WA, *et al.* Formulation, optimization, and nephrotoxicity evaluation of an antifungal in situ nasal gel loaded with voriconazole--clove oil transferosomal nanoparticles. Drug Deliv 2021; 28:2229–2240.
41. Balakrishnan P, Park E-K, Song C-K, Ko H-J, Hahn T-W, Song K-W, *et al.* Carbopol-incorporated thermoreversible gel for intranasal drug delivery. Molecules 2015; 20:4124–4135.
42. dos Santos ACM, Akkari ACS, Ferreira IRS, Maruyama CR, Pascoli M, Guilherme VA, *et al.* Poloxamer-based binary hydrogels for delivering tramadol hydrochloride: sol-gel transition studies, dissolution-release kinetics, *in vitro* toxicity, and pharmacological evaluation. Int J Nanomedicine 2015; 10:2391–2401.
43. Şenyiğit ZA, Karavana SY, İlem-Özdemir D, Çalışkan Ç, Waldner C, Şen S, *et al.* Design and evaluation of an intravesical

delivery system for superficial bladder cancer: Preparation of gemcitabine HCl-loaded chitosan-thioglycolic acid nanoparticles and comparison of chitosan/poloxamer gels as carriers. Int J Nanomedicine 2015; 10:6493–6507.
44. Bhandwalkar MJ and Avachat AM. Thermoreversible nasal *in situ* gel of venlafaxine hydrochloride: Formulation, characterization, and pharmacodynamic evaluation. AAPS PharmSciTech 2013; 14:101–110.
45. Kushan E and Senses E. Thermoresponsive and injectable composite hydrogels of cellulose nanocrystals and pluronic F127. ACS Appl Bio Mater 2021; 4:3507–3517.
46. Zou S, He Q, Wang Q, Wang B, Liu G, Zhang F, *et al.* Injectable nanosponge-loaded Pluronic F127 hydrogel for pore-forming toxin neutralization. Int J Nanomedicine 2021; 4239–4250.
47. Yurtda\cs-K\ir\iml\io\uglu G. A promising approach to design thermosensitive in situ gel based on solid dispersions of desloratadine with Kolliphor®188 and Pluronic®F127. J Therm Anal Calorim 2022; 147:1307–1327.
48. Rao M, Agrawal DK, and Shirsath C. Thermoreversible mucoadhesive in situ nasal gel for treatment of Parkinson's disease. Drug Dev Ind Pharm 2017; 43:142–150.
49. Verhoeven E, Vervaet C, and Remon JP. Xanthan gum to tailor drug release of sustained-release ethylcellulose mini-matrices prepared via hot-melt extrusion: *In vitro* and *in vivo* evaluation. Eur J Pharm Biopharm 2006; 63:320–330.
50. Charoo NA, Kohli K, Ali A. Preparation of *in situ*-forming ophthalmic gels of ciprofloxacin hydrochloride for the treatment of bacterial conjunctivitis: *In vitro* and *in vivo* studies. J Pharm Sci 2003; 92:407–413.
51. Mahmoud RA, Abdelhafez WA, Mahmoud EA, Hassan Y, Amin MA, Zayed GM, *et al.* Cilostazol niosomes-loaded transdermal gels: An *in vitro* and *in vivo* anti-aggregant and skin permeation activity investigations towards preparing an efficient nanoscale formulation. Nanotechnol Rev 2024; 13:20240066.
52. Bosman A, Koek WNH, Campos-Obando N, van der Eerden BCJ, Ikram MA, Uitterlinden AG, *et al.* Sexual dimorphisms in serum calcium and phosphate concentrations in the Rotterdam Study. Sci Rep 2023; 13:8310-8319.
53. Pardhe BD, Pathak S, Bhetwal A, Ghimire S, Shakya S, Khanal PR, *et al.* Effect of age and estrogen on biochemical markers of bone turnover in postmenopausal women: A population-based study from Nepal. Int J Womens Health 2017; 9:781–788.
54. Shu J, Tan A, Li Y, Huang H, and Yang J. The correlation between serum total alkaline phosphatase and bone mineral density in young adults. BMC Musculoskelet Disord 2022; 23:467-474.
55. Cheng X and Zhao C. The correlation between serum levels of alkaline phosphatase and bone mineral density in adults aged 20 to 59 years. Medicine (Baltimore) 2023; 102:e34755.
56. Ahmed OA and Badr-Eldin SM. *In situ* misemgel as a multifunctional dual-absorption platform for nasal delivery of raloxifene hydrochloride: Formulation, characterization, and *in vivo* performance. Int J Nanomedicine 2018; 13:6325–6335.
57. Saini D, Fazil M, Ali MM, Baboota S, and Ali J. Formulation, development and optimization of raloxifene-loaded chitosan nanoparticles for treatment of osteoporosis. Drug Deliv 2015; 22:823–836.
58. Moreno E, Schwartz J, Larrañeta E, Nguewa P, Sanmartín C, Agüeros M, *et al.* Thermosensitive hydrogels of poly(methyl vinyl ether-co-maleic anhydride) - Pluronic (R) F127 copolymers for controlled protein release. Int J Pharm 2014; 459:1-9.
59. Varshosaz J, Hassanzadeh F, Sadeghi-aliabadi H, Larian Z, Rostami M. Synthesis of Pluronic® F127-poly (methyl vinyl ether-alt-maleic acid) copolymer and production of its micelles for doxorubicin delivery in breast cancer. Chem Eng J 2014; 240:133–146.